### Title

Formation of 3D Self-Organized Neuron-Glial Interface Derived from Neural Stem Cells via Mechano-Electrical Stimulation




### Journal

Advanced Healthcare Materials, 10(19)

### ISSN

2192-2640



### Authors

Tai, Youyi
Ico, Gerardo
Low, Karen
et al.



### Publication Date

2021-10-01

### DOI

10.1002/adhm.202100806

Peer reviewed

WILEY-VCH

# Formation of 3D self-organized neuron-glial interface derived from neural stem cells via mechano-electrical stimulation

Youyi Tai[1#], Gerardo Ico[1#], Karen Low[1#], Junze Liu[1], Tanvi Jariwala[1], David Garcia-Viramontes[1], Kyu Hwan Lee[2], Nosang V. Myung[3], B. Hyle Park[1], Jin Nam[1]*

[1]Department of Bioengineering
University of California, Riverside
Riverside, CA 92521, USA

[2]Korea Institute of Materials Science
797 Changwondaero, Seongsan gu
Changwon, Gyeongnam, South Korea

[3]Department of Chemical and Biomolecular Engineering
University of Notre Dame
Notre Dame, IN 46556, USA

#: equally contributed

*: corresponding author
Jin Nam, Ph.D.
Department of Bioengineering
University of California, Riverside
Riverside, CA 92521
E-mail: jnam@engr.ucr.edu
Tel: 951-827-2064

Keywords: neuromodulation, piezoelectric nanofibers, neural stem cells, mechano-electrical stimulation

**Abstract**

Due to dissimilarities in genetics and metabolism, current animal models cannot accurately depict human neurological diseases. To develop patient-specific *in vitro* neural models, a functional material-based technology that offers multi-potent stimuli for enhanced neural tissue development is devised. An electrospun piezoelectric poly(vinylidene fluoride-trifluoroethylene) (P(VDF-TrFE)) nanofibrous scaffold is systematically optimized to maximize its piezoelectric properties while accommodating the cellular behaviors of neural stem cells. Hydro-acoustic actuation is elegantly utilized to remotely activate the piezoelectric effect of P(VDF-TrFE) scaffolds in a physiologically-safe manner for the generation of cell-relevant electric potentials. This mechano-electrical stimulation, which arose from the deflection of the scaffold and its consequent generation of electric charges on the scaffold surface under hydro-acoustic actuation, induces the multi-phenotypic differentiation of neural stem cells simultaneously towards neuronal, oligodendrocytic, and astrocytic phenotypes. As compared to the traditional biochemically-mediated differentiation, the three-dimensional neuron-glial interface induced by the mechano-electrical stimulation results in enhanced interactions among cellular components, leading to superior neural connectivity and functionality. These results demonstrate the potential of piezoelectric material-based technology for developing functional neural tissues *in vitro* via effective neural stem cell modulation with multi-faceted regenerative stimuli.

## 1. Introduction

While the size of the elderly population afflicted by various neurodegenerative diseases is exponentially increasing, advances in effective treatments are limited due to a lack of appropriate developmental tools. Current animal models often fall short in replicating true neurological diseases in humans due to dissimilarities in genetics and metabolism as compared to human pathologies that are heavily dependent on individual genetics.[1] Therefore, the development of patient-specific *in vitro* nerve models is essential to enhance our fundamental understanding of the pathogenesis of prevalent neurological diseases/disorders.[2] This may lead to discovering efficient therapeutic interventions that are not often attainable with current animal models. However, the inherent complexity of neural structures, which the use of typical biochemical/pharmaceutical agents is not sufficient to achieve, has limited the development of *in vitro* models that depict the functional characteristics of the native tissue.

In this regard, exogenous physical stimuli have been shown to augment typical biochemical stimulation on neural development/regeneration. Electrical stimulation has gained attention as an effective regenerative signal to enhance nerve regeneration by modulating the electro-responsiveness of neural cells, including the auto-regulation of neurotrophic factors.[3] Specifically, studies have demonstrated that local surface electrical charges created by bioelectric fields induce the secretion of various growth factors from neural cells to promote nerve fiber outgrowth[3-4]. In addition, electrical stimulation has been shown to modulate neural stem cell differentiation toward neurons.[5] *In vivo*, applied electric fields have been shown to accelerate nerve regeneration in both the peripheral nervous system (PNS) and central nervous system (CNS).[6] Conductive materials, especially mechanically compliant polymers such as polyaniline, polypyrrole, and polythiophene, have shown promising potential as interfacial materials to electrically stimulate neural cells for functional neural tissue engineering and nerve regeneration.[7] However, the application of conductive polymer scaffolds in *in vitro* nerve

models is not appropriate because the materials' intrinsic electrical conductivity will likely disrupt native nerve signal transduction once the engineered tissue is fully mature.

In this regard, piezoelectric materials provide a means to electrically stimulate adherent cells without interfering with innate electrical signal transduction. Piezoelectric materials generate surface potentials under dynamic mechanical strain while remaining electrically insulating under static conditions. The mechanical perturbation that materializes the piezoelectric effect also exerts mechanical stimulation, another physical stimulus, directly to cells. Intracellular calcium levels, essential for regulating neuronal functions, are modulated by mechanical stimulation via stretch-activated ion channels.[8] For glial cells, the application of pulsed ultrasound promotes Schwann cell proliferation, resulting in accelerated peripheral nerve regeneration.[9] The differentiation of neural stem cells is also affected by their mechanical environment,[10] further suggesting the important role of mechanical stimulation in neural tissue development/regeneration.

Several studies have attempted to utilize biocompatible piezoelectric polymers, such as poly(vinylidene fluoride) (PVDF) or its derivatives including poly(vinylidene fluoride-trifluoroethylene) (P(VDF-TrFE)), for nerve regeneration *in vitro* as well as *in vivo*. PVDF has been shown to promote neurite elongation of dorsal root ganglia cells, stimulate the secretion of neurotrophic factors from Schwann cells, and induce differentiation of neural stem cells towards neurons.[11] An *in vivo* study demonstrated that an implanted P(VDF-TrFE) conduit was able to bridge a short nerve gap to restore partial functionality.[12] Although those pioneering studies showed favorable phenomenological observations from the use of PVDF derivatives, the lack of systematic piezoelectric characterization and proper activation may have limited the realization of its full potential.

In this study, electrospun P(VDF-TrFE) nanofibers were employed as a cell culture scaffold for mouse and human neural stem cells (mNSCs and hNSCs, respectively) to

demonstrate the regenerative effects of electrical stimulation, mechanical stimulation, or the combination of both. Based on the systematic functional characterization of the piezoelectric scaffolds, we engineered a cell culture system that enables the electrical stimulation of neural stem cells using the piezoelectric activation of the scaffolds in a physiologically safe manner. The hydro-acoustic actuation used to realize the piezoelectric effect of the scaffolds also provided another means of physically stimulating the cells. We demonstrate that the mechano-electrical stimulation, derived from the hydro-acoustic actuation of the piezoelectric scaffold, induces the multi-phenotypic differentiation of neural stem cells to form a neuron-glial interface, resulting in enhanced neural functionalities as compared to a traditional biochemically mediated differentiation scheme. Therefore, this study provides a key step towards developing functionally competent *in vitro* nerve models via effective neural cell modulation with a piezoelectric material-based platform.

## 2. Results

In this study, electrospinning was utilized to synthesize polymeric nanofibrous scaffolds of biocompatible, piezoelectric PVDF derivatives to tune their morphological and piezoelectric characteristics as a cell culture platform for functional neural tissue formation. As we have previously demonstrated, the fiber diameter of electrospun P(VDF-TrFE) nanofibers determines their piezoelectric performance as smaller fiber diameters exponentially enhance the piezoelectric constant $d_{33}$.[13] However, the fiber size has also been shown to significantly affect cellular behaviors including the degree of neural stem cell alignment that promotes neurite formation/elongation on larger fibers by restricting cell spreading.[14] To optimize the electrospun fiber diameter that achieves a balance between enhanced piezoelectric properties while promoting the cellular alignment, P(VDF-TrFE) was electrospun to produce three different fiber diameters. Electrospinning conditions, including polymer concentration,

solution viscosity, flow rate, spinneret-to-collector distance, temperature, and humidity were fine-tuned to reproducibly synthesize uniform aligned P(VDF-TrFE) nanofibers having average fiber diameters of 200, 500, and 800 nm (**Figure 1A**). Fibers with a larger average diameter exhibited a greater degree of alignment, however, all scaffolds showed relatively high fiber alignment within 20° of the neutral axis (**Figure 1B**).

The fiber size-dependent piezoelectric performance of the electrospun aligned P(VDF-TrFE) nanofibers was determined by subjecting the samples to a vertical actuator at 3 Hz in an aqueous condition (**Figure S1**). A hollow chamber filled with an aqueous solution was used to hold a strip of the P(VDF-TrFE) nanofiber mat that is subjected to hydro-acoustic actuation, created by a periodic vertical translational movement (**Figure 1C**). When the stage moves down, it induces upward deflection of the P(VDF-TrFE) mat, leading to the transient development of electric potentials across the thickness of the mat. The polarity of the electric potential depends on the direction of the deflection, thereby a complete cycle of up and down translational motions of the chamber produces the characteristic piezoelectric double peaks. With a maximum applied energy flux of $1.226\times10^{-4}$ mJ mm$^{-2}$, the P(VDF-TrFE) mats generated electric potentials whose magnitudes depend on the nanofiber diameter and nanofiber mat thickness (**Figure S2-4**). As expected from our previous study that demonstrated the fiber size-dependency of piezoelectric constants in electrospun P(VDF-TrFE) nanofibers,[15] the smallest fiber diameter with a similar mat thickness generated the highest peak-to-peak voltage outputs under a similarly applied strain (**Figure 1D**). The potential generation from the P(VDF-TrFE) mats increased as the mat thickness increased for all fiber sizes (**Figure 1E**). These results provided a method to tune the morphological properties of the P(VDF-TrFE) nanofiber mats (i.e., fiber diameter and mat thickness) accordingly for desired piezoelectric performance in the subsequent experiments.

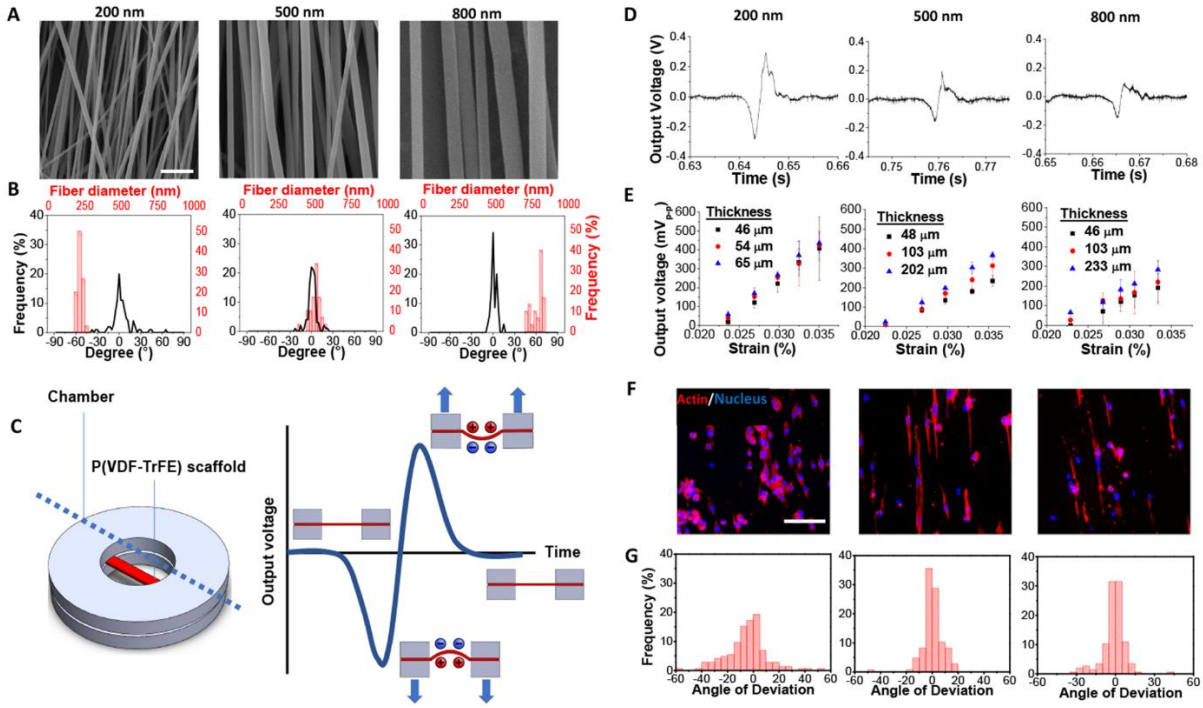


**Figure 1. Morphological and piezoelectric characterization of electrospun aligned P(VDF-TrFE) nanofibers with various fiber diameters and their effects on neural stem cell alignment.** (**A**) SEM images of electrospun aligned P(VDF-TrFE) nanofibers with various average fiber diameters and (**B**) histograms of fiber diameter and alignment (scale bar = 2 μm, n=150 from 3 independent samples). (**C**) Schematic diagram depicting the hollow-cylindrical, scaffold-holding chamber that allows deflection of the electrospun aligned P(VDF-TrFE) nanofiber mat under hydro-acoustic actuation generated by a periodic vertical translational motion of the chamber. The nanofiber mat deflection, depicted in the cross-sectional view (following the dotted line) of the mat/chamber construct, induces the transient development of electric potentials across the thickness of the P(VDF-TrFE) nanofiber mat, where their polarity depends on the direction of the deflection. Arrows indicate the direction of the chamber movement. (**D**) The characteristic electric response of the electrospun aligned P(VDF-TrFE) nanofiber mats with an average fiber diameter of approximately 200, 500, or 800 nm (from left to right) and a fiber mat thickness of approximately 200 μm under hydro-acoustic actuation at an applied strain of 0.033%. (**E**) Peak-to-peak voltage outputs of the electrospun aligned P(VDF-TrFE) nanofiber mats with various fiber diameters (200, 500, or 800 nm (from left to right)) and mat thicknesses with respect to different magnitudes of the applied strain. Data are presented as average ± standard deviation (n=10). (**F**) Immunofluorescence images of mouse neural stem cells cultured on the electrospun aligned P(VDF-TrFE) nanofiber mats for 96 hours and (**G**) orientation histograms of the cells on the scaffolds with an average fiber diameter of (**F/G** left) 200, (**F/G** middle) 500, and (**F/G** right) 800 nm (red: actin (phalloidin), blue: nucleus (DAPI), scale bar = 100 μm; n=150 cells in 15 different images from 3 independent samples).

We then evaluated the effects of fiber diameter on mNSC behaviors as their alignment is guided by fiber diameter (**Figure 1F, G**). When statically cultured, mNSCs exhibited greater alignment on the P(VDF-TrFE) nanofiber mats with 500 and 800 nm fiber diameters that likely prevented the cells from spreading across adjacent fibers as compared to 200 nm fiber size.

The greater alignment of the cells on larger fiber diameters positively affected NSC elongation. To balance the superior piezoelectric performance of the smaller fiber and the desirable neural stem cell behaviors on the larger fiber, electrospun P(VDF-TrFE) nanofiber mats with an average fiber diameter of 500 nm were utilized for the remainder of the study.

In order to systematically analyze the contribution of scaffold-generated electric potentials on cells, decoupled from the hydro-acoustic actuation that was utilized to activate the piezoelectric effect of the piezoelectric nanofiber mats, a thermally inactivated form of electrospun aligned PVDF nanofibers was synthesized. Since the piezoelectric stabilizer, trifluoroethylene (TrFE) prevents the suppression of piezoelectric properties in P(VDF-TrFE), PVDF that presents similar surface chemistry yet distinctive piezoelectric properties was used. Electrospinning parameters were optimized to produce aligned PVDF nanofibers with similar fiber diameter and a degree of fiber alignment to those of aligned P(VDF-TrFE) nanofibers. Differential scanning calorimetry (DSC) was utilized to determine the proper heat-treatment temperature for 1) the piezoelectric enhancement of electrospun aligned P(VDF-TrFE) nanofibers and 2) the piezoelectric inactivation of electrospun aligned PVDF nanofibers. To enhance the piezoelectricity in the electrospun aligned P(VDF-TrFE) nanofibers, thermal treatment below the Curie temperature (114.9 °C) at 90 °C was carried out to promote the slight re-arrangement of the crystalline polarized domains without causing a full transition from the ferro- to para-electric phase (**Figure 2A**).[13] The piezoelectric inactivation of electrospun aligned PVDF nanofibers requires proper thermal treatment; the electrospinning process intrinsically subjects the polymer to mechanical stretching and electrical biasing, which results in the induction of piezoelectricity in PVDF. The DSC curve shows a tight temperature window near 158 °C for the phase transition of the piezoelectric β-phase towards the non-piezoelectric α-phase. We utilize this temperature regimen to inactivate the piezoelectric properties of electrospun aligned PVDF nanofibers while not completely melting the fibrous structure

(**Figure 2B**).[16] Both thermal treatments, 90 °C for 24 hrs for electrospun aligned P(VDF-TrFE) nanofibers and 158°C for 1 hr for electrospun aligned PVDF nanofibers, have no effect on the morphology of the nanofibers (**Figure 2C, D**). The thermally treated P(VDF-TrFE) nanofibers exhibited an enhanced piezoelectric coefficient of -37 ± 4 pm $V^{-1}$, as compared to -32 ± 3 pm $V^{-1}$ of the as-spun form (**Figure 2E**). In comparison, the piezoelectric inactivation of electrospun aligned PVDF nanofibers was confirmed by piezo-response force microscopy (PFM), which showed a substantial reduction in the piezoelectric coefficient, $d_{33}$, from the as-spun PVDF nanofibers at -31 ± 8 pm $V^{-1}$ to a negligible value of -6 ± 2 pm $V^{-1}$ in the thermally inactivated PVDF nanofibers (**Figure 2F**).

Electrical properties of these thermally treated nanofiber mats were measured using the hydro-acoustic actuation system as described earlier **(Figure S1**). The effects of the thermal treatment were evident from the substantial reduction of potential generation in the thermally treated, electrospun aligned PVDF nanofiber mats (hereinafter piezo-inactivated scaffolds) under a periodic hydro-acoustic actuation, as compared to the that in the thermally treated, electrospun aligned P(VDF-TrFE) nanofiber mats (hereinafter piezoelectric scaffolds) (**Figure 2G, H**). As a function of applied strain, the peak-to-peak voltage was proportionally generated at the surface of the thermally treated, electrospun aligned P(VDF-TrFE) nanofiber mats (**Figure 2G**). In contrast, due to the thermal inactivation, a negligible voltage was generated from the thermally treated, electrospun aligned PVDF nanofiber mats up until 0.03% strain (**Figure 2H**).

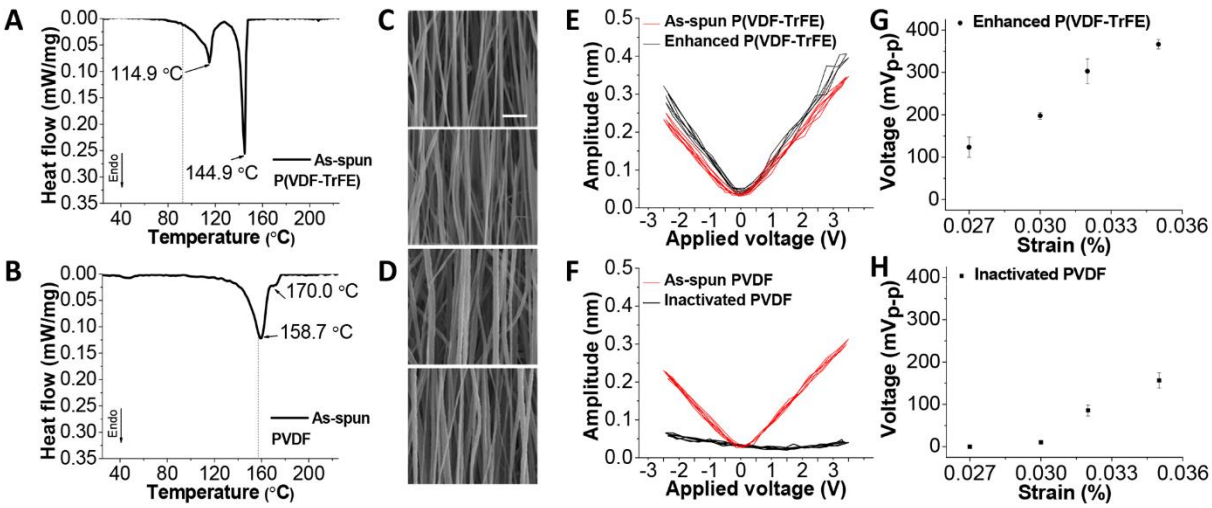


**Figure 2. Piezoelectric characterization of thermally enhanced electrospun aligned P(VDF-TrFE) and thermally inactivated electrospun aligned PVDF scaffolds.** Differential scanning calorimetry (DSC) curves of (**A**) electrospun aligned P(VDF-TrFE) nanofibers to determine the Curie and melting temperature at approximately 114.9 and 144.9 °C, respectively, as compared to (**B**) electrospun aligned PVDF nanofibers exhibiting a tight window of temperature transition from the electroactive phase (β-phase, approximately 158.7 °C) to piezoelectric-less α-phase and melting approximately at 170.0 °C. (**C**) SEM images of as-spun aligned P(VDF-TrFE) nanofibers (top) and 90 °C thermally enhanced, electrospun aligned P(VDF-TrFE) nanofibers (bottom). (**D**) SEM images of as-spun aligned PVDF nanofibers (top) and 158 °C thermally inactivated, electrospun aligned PVDF nanofibers (bottom). (scale bar = 5 μm). (**E**, **F**) Piezoresponse graphs of individual P(VDF-TrFE) and PVDF nanofibers showing the piezoelectric enhancement of P(VDF-TrFE) (approximately 483 nm fiber diameter) and the piezoelectric inactivation of PVDF nanofibers (approximately 469 nm) by the thermal treatments, as compared to the as-spun nanofibers (approximately 509 nm P(VDF-TrFE) and 497 nm PVDF nanofibers). (**G**, **H**) Peak-to-peak voltage generation of (**G**) thermally enhanced electrospun aligned P(VDF-TrFE) and (**F**) thermally inactivated electrospun aligned PVDF nanofibrous scaffolds, having a similar thickness of approximately 200 μm, with respect to the applied strain. Data are presented as average ± standard deviation (n=10).

To determine an appropriate regimen of electrical stimulation for enhanced neural stem cell behaviors, mNSCs were subjected to externally applied AC voltages with a similar electric pulse profile to the hydro-acoustically generated voltages from the piezoelectric scaffolds (**Figure 3 and S5**). As the magnitude of electrical stimulation increased from 0 (control) to 200 $mV_{p-p}$, mNSCs exhibited increased neuronal differentiation. However, a high magnitude of 300 $mV_{p-p}$ resulted in the decreased numbers of total cells and neurons, likely due to damages from the electrical stimulation. A live & dead cell assay was performed after the first application of electrical stimulation with various magnitudes and the result confirmed a significant decrease

of cell viability under the application of 300 $mV_{p-p}$, corroborating with the data in **Figure 3F** (**Figure S6**). To balance the better cell viability at a low magnitude of electrical stimulation and the desirable neuronal differentiation behavior at a higher electrical output, 200 $mV_{p-p}$ was determined as the optimal stimulation regimen. Thus, a strain of 0.03% to produce approximately 200 $mV_{p-p}$ from the piezoelectric scaffolds and an insignificant voltage from the piezo-inactivated scaffolds as shown in **Figure 2G, H** was chosen for all subsequent studies.

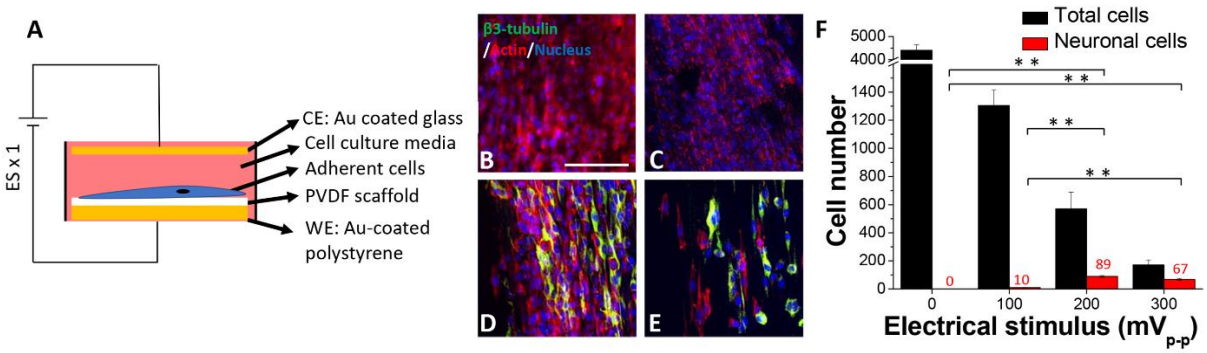


**Figure 3. Effects of direct electrical stimulation on neural stem cells.** (**A**) Schematic diagram depicting a cross-sectional view of a cell culture device in a 12-well plate format to deliver direct electrical stimulation with various AC voltages. Immunofluorescence images of mouse neural stem cells (mNSCs) cultured on thermally inactivated electrospun aligned PVDF scaffold and exposed to (**B**) 0, (**C**) 100, (**D**) 200, or (**E**) 300 $mV_{p-p}$ and (**F**) the average number of total cells (black bar) and neurons (red bar) in a cell culture area of 1.3 mm x 1 mm (green: β3-tubulin (neuronal marker), red: actin (phalloidin), blue: nucleus (DAPI); n=15 images from 3 independent samples, **: $p < 0.01$; error bars indicate the standard error of the mean).

By utilizing these piezoelectric and piezo-inactivated scaffolds, we examined the effects of electrical stimulation (ES: cells cultured on the piezo-inactivated scaffolds with direct electrical stimulation), mechanical stimulation (MS: cells cultured on the piezo-inactivated scaffolds with hydro-acoustic actuation), or mechano-electrical stimulation (MES: cells cultured on the piezoelectric scaffolds with hydro-acoustic actuation) on the differentiation capacity of mNSCs towards neuronal, oligodendrocytic, or astrocytic cells (**Figure 4**). The gene expression of *Tubb3*, an early neuronal marker, was significantly enhanced regardless of the stimulation type as compared to the control group where cells were statically cultured in tissue culture plates. While the intermediate neuronal marker, *Map2*, was significantly

upregulated by mechano-electrical stimulation, the expression of a mature neuronal marker, *Eno2*, was significantly upregulated in both ES and MES conditions (**Figure 4A-C**). Protein expression of β3-tubulin under various culture conditions corroborates with those found in the gene expression study (**Figure 4D-F**). All scaffolds showed some expression of the neuronal marker (**Figure 4D-F, Figure S7A, B**) likely due to the aligned morphology of the scaffolds inducing neuronal differentiation of the cells. The cells in the MES condition showed, however, the formation of longer extended neurites, indicating more developmentally mature neurons. In contrast to neuronal differentiation, *Olig1* and *Cldn11*, intermediate markers for neural stem cell differentiation towards oligodendrocyte, were significantly upregulated by the application of mechanical stimulation as in both the MS and MES conditions (**Figure 4G, H**). *Mog*, expressed on the outermost surface of myelin sheaths indicating more mature oligodendrocytes, however, was significantly upregulated in the MES condition, showing a developmental stage-dependent effect of mechano-electrical stimulation (**Figure 4I**). Similarly, the protein expression of MBP (myelin basic protein) was only observed in the cells in the MES group, supporting the notion that electrical stimulation in the presence of mechanical stimulation, promotes mNSC differentiation and maturation towards myelinating oligodendrocytes (**Figure 4J-L, Figure S7C, D**). In regards to the differentiation of mNSCs towards the astrocyte phenotype, a similar expression pattern to oligodendrocytic differentiation was observed. Significant upregulation was observed in the MS and MES conditions for early/intermediate astrocytic genes, *Aldh1l1* and *Cspg4*, while the piezoelectric material-mediated mechano-electrical stimulation enhanced the expression of *Gfap*, an astrocytic functional marker (**Figure 4M-O**). At the protein level, the expression of EAAT2, an astrocyte-selective glutamate transporter, was observed only in the MES condition, signifying the potency of the mechano-electrical stimulation on the astrocytic maturation of NSCs (**Figure 4P-R, Figure S7E, F**).

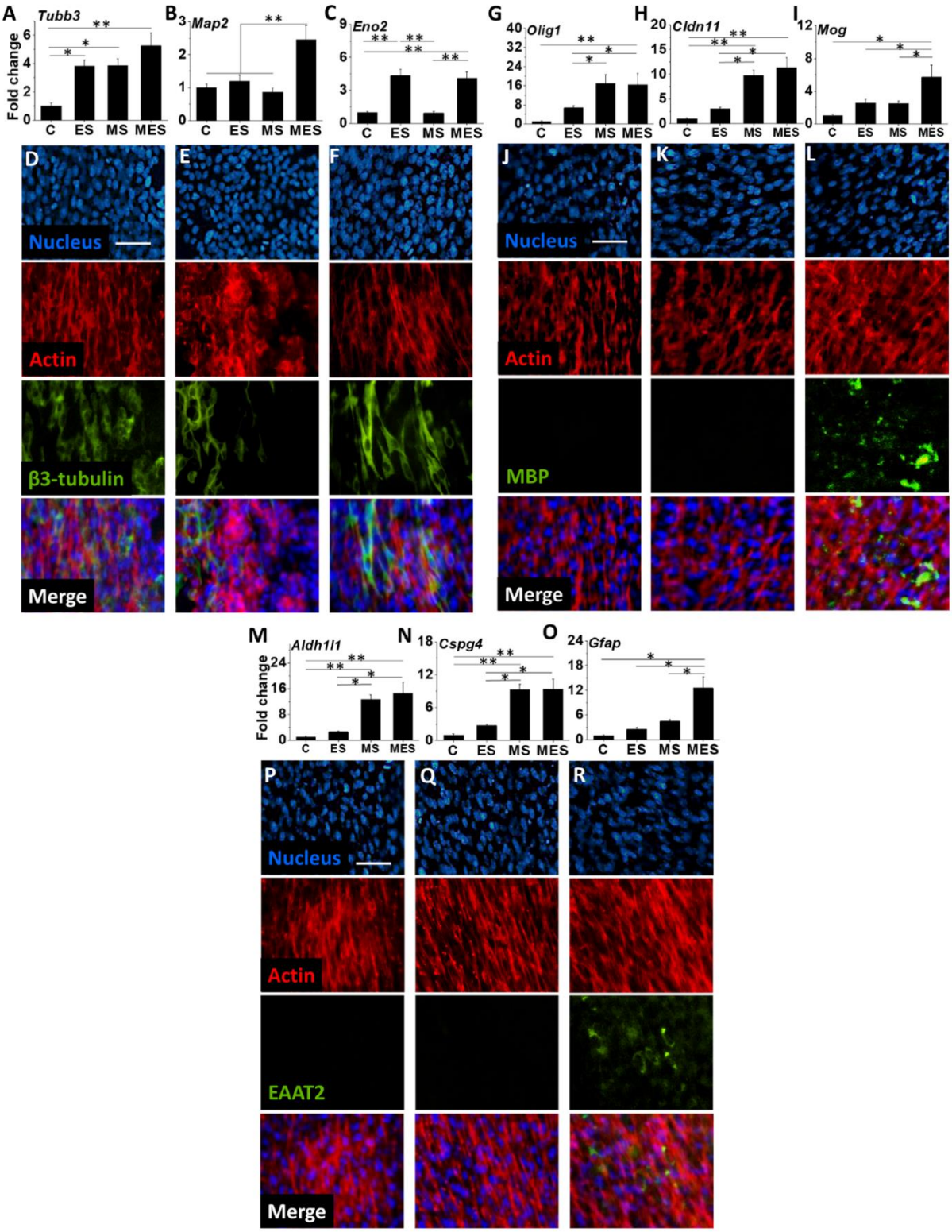


**Figure 4. Effects of piezoelectric P(VDF-TrFE) scaffold-mediated mechano-electrical stimulation on multi-phenotypic differentiation of mouse neural stem cells.** For electrical stimulation (ES) condition, cells were pre-cultured on thermally inactivated electrospun aligned PVDF scaffolds (piezo-inactivated scaffolds) for 2 days prior to being exposed to 200 $mV_{p-p}$ electrical stimulation (2 hrs/day) for subsequent 5 days. For mechanical stimulation (MS) and mechano-electrical (MES) conditions, cells were pre-cultured on the thermally

inactivated scaffolds and electrospun aligned P(VDF-TrFE) scaffolds (piezoelectric scaffolds), respectively, for 2 days prior to being subjected to hydro-acoustic actuation (2 hrs/day) for subsequent 5 days. Gene expression of neuronal markers, (**A**) *Tubb3*, (**B**) *Map2*, and (**C**) *Eno2*, oligodendrocytic markers, (**G**) *Olig1*, (**H**) *Cldn11*, and (**I**) *Mog* and astrocytic markers, (**M**) *Aldh1l1*, (**N**) *Cspg4*, and (**O**) *Gfap* after a total culture duration of 1 week under various conditions. mNSCs cultured statically on tissue culture plate served as controls (C, n = 6, * and ** denote statistical significance of $p < 0.05$ and $p < 0.01$, respectively; error bars indicate the standard error of the mean). Immunofluorescence images for the expression of (**D**-**F**) a neuronal marker β3-tubulin, (**J**-**L**) an oligodendrocytic marker MBP and (**P**-**R**) an astrocytic marker EAAT2 from mNSCs subjected to electrical stimulation (**D, J, P**), mechanical stimulation (**E, K, Q**) and mechano-electrical stimulation (**F, L, R**) (scale bar=25 μm).

To evaluate the morphological development of the engineered nerve construct, mNSCs or hNSCs were cultured on the piezoelectric scaffolds for 3 weeks with or without the hydro-acoustic actuation. The results from mNSCs were utilized to test their reproducibility in human cells in the rest of the study due to their greater relevance to the physiology/pathology of human neurological diseases, which are strongly influenced by genetics. Under the static culture condition, confocal 3D reconstruction showed that the cells predominantly differentiated to neurons, evident from the expression of NeuN, a neuronal marker, and a lack of ALDH1L1 or $O_4$ expression, markers for astrocytes and oligodendrocytes, respectively (**Figure 5A, B** (**from Video S1A, S1B**) and **Figure 6A, B** (**Video S2A, S2B**)). In contrast, mechano-electrical stimulation induced the formation of a layered structure, composed of multi-phenotypic cells, where NeuN-positive cells were localized at the top layer of the cellular structure while ALDH1L1 and $O_4$ were expressed in the cells near the scaffold surface (**Figure 5D, E** (**Video S1D, S1E**) and **Figure 6D, E** (**Video S2D, S2E**)). The expression of astrocyte marker GFAP and oligodendrocyte marker $O_4$ clearly shows the potency of the mechano-electrical stimulation on glial phenotype development **(Figure 5C, F** (**Video S1C, S1F**) and **Figure 6C, F** (**Video S2C, S2F**)). Single oblique sections obtained from confocal z-stacks confirm the thickness-dependent layered cellular structure, composed of heterogeneous populations of neurons, astrocytes, and oligodendrocytes in the mechano-electrical condition (**Figure 5G-L** and **Figure 6G-L**). Interestingly, the quantification of these heterogeneous cell populations

with respect to the thickness of the engineered nerve construct demonstrates that a mixture of astrocytic and oligodendrocytic cells forms under a layer of neurons (**Figure 5M, N,** and **Figure 6M, N**).

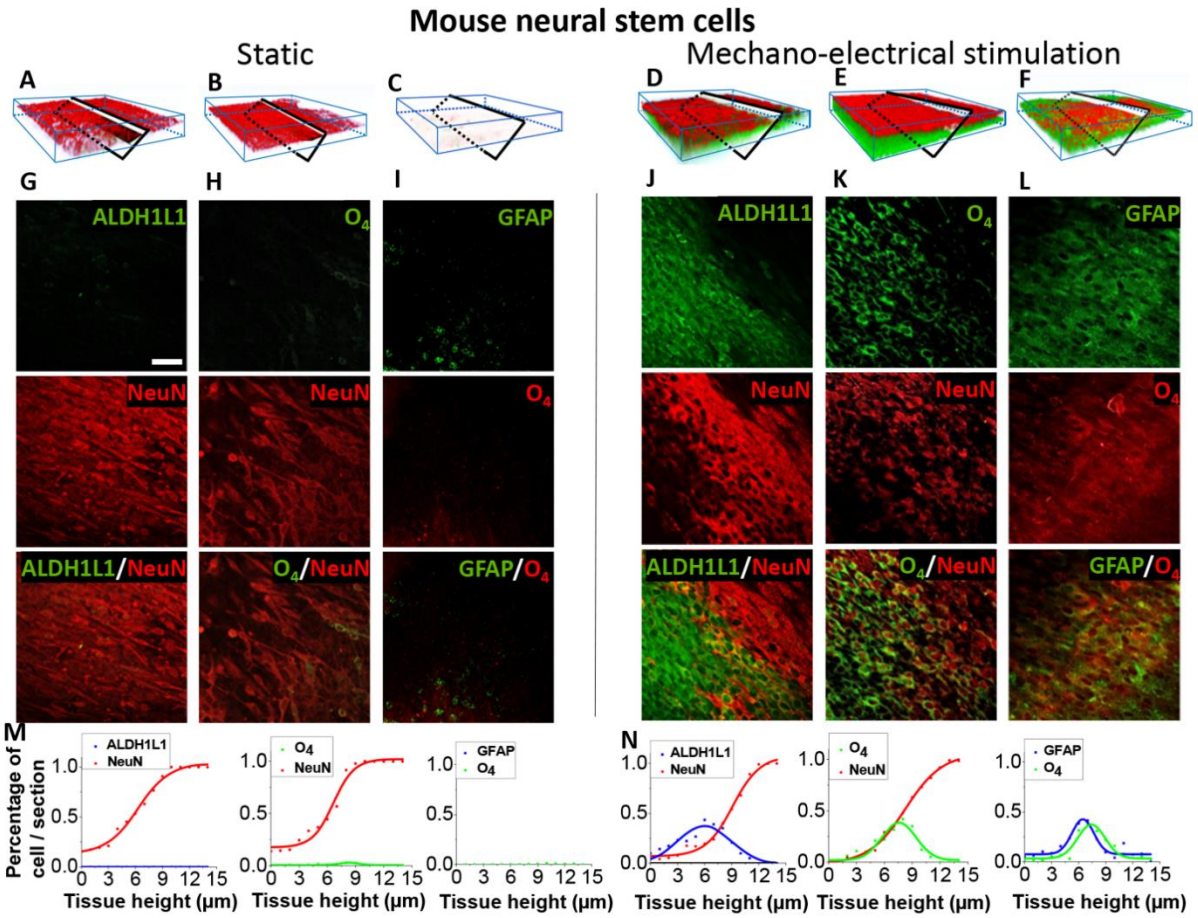


**Figure 5. 3D neuron-glial interface formation of mouse neural stem cells induced by piezoelectric P(VDF-TrFE) scaffold-mediated mechano-electrical stimulation.** (**A-F**) Confocal z-stack imaging with (**A, D**) anti-NeuN (neuronal marker; red) and anti-ALDH1L1 (astrocytic marker; green), (**B, E**) anti-NeuN (red), and anti-O4 (oligodendrocytic marker; green) or (**C, F**) anti-O4 (red), and anti-GFAP (astrocytic marker; green). As compared to statically cultured cells that predominantly differentiated to neurons (**A-C**), confocal 3D reconstruction of hydro-acoustically actuated cell/scaffold constructs (mechano-electrical stimulation) (**D-F**) showed a multi-phenotypic differentiation behavior, resulting in the formation of a multilayered cellular structure. (**G-L**) Single oblique sections (indicated in **A-F**) from each 3D confocal image of (**G-I**) static and (**J-L**) actuated conditions showing the formation of multi-phenotypic cellular interfaces under the mechano-electrical stimulation (scale bar=100 μm). (**M, N**) Quantitative analysis of confocal images showing the depth-dependent distributions of neuronal and glial cells (**M**) without or (**N**) with the mechano-electrical stimulation. Each graph used three confocal Z-stack images from independent samples. For the mechano-electrical stimulation condition, mouse neural stem cells (mNSCs) were pre-cultured on the piezoelectric scaffolds for 2 days prior to being subjected to hydro-acoustic actuation (2 hrs/day) for a subsequent 19 days. Cells cultured on the piezoelectric scaffolds without being subjected to hydro-acoustic actuation served as static controls.

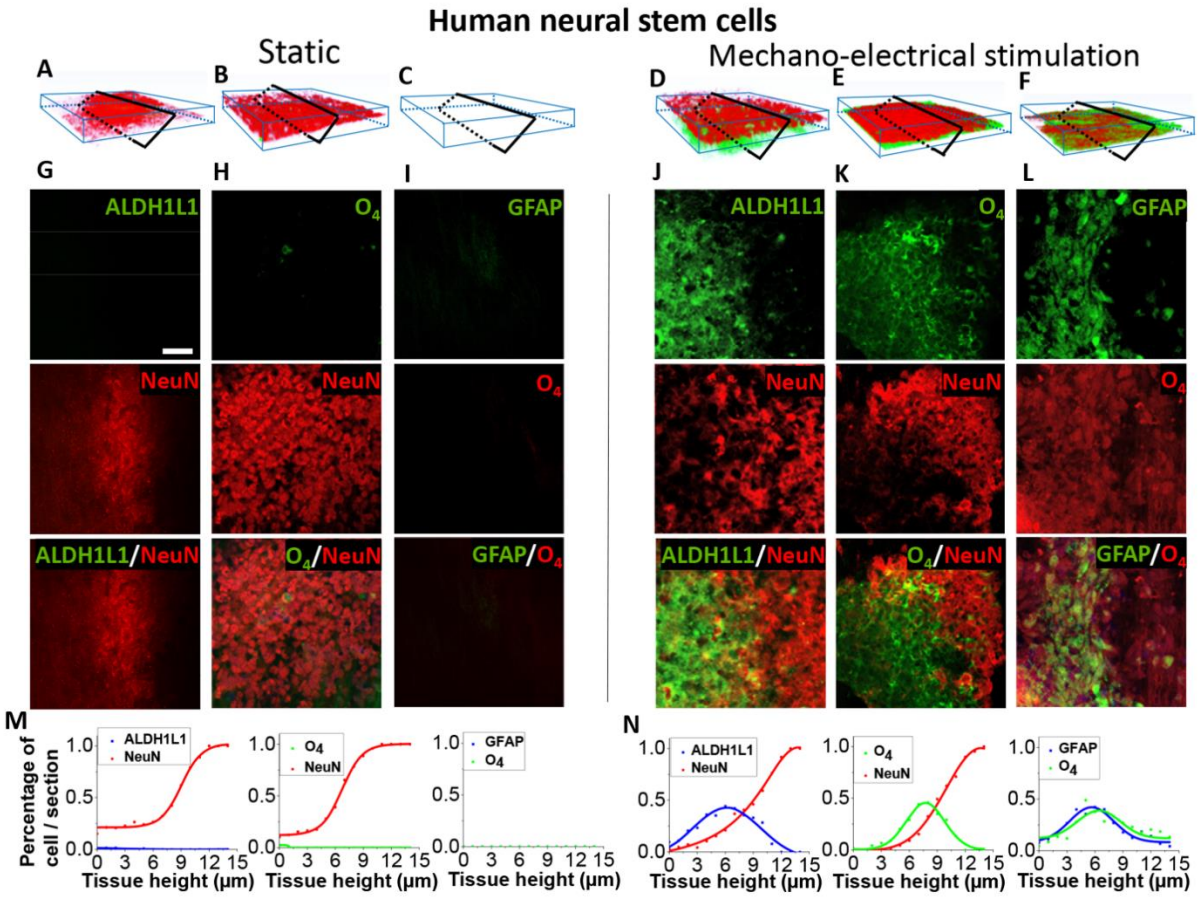


**Figure 6. 3D neuron-glial interface formation of human neural stem cells induced by piezoelectric P(VDF-TrFE) scaffold-mediated mechano-electrical stimulation.** (**A-F**) Confocal z-stack imaging with (**A, D**) anti-NeuN (neuronal marker; red) and anti-ALDH1L1 (astrocytic marker; green), (**B, E**) anti-NeuN (red), and anti-$O_4$ (oligodendrocytic marker; green) or (**C, F**) anti-$O_4$ (red), and anti-GFAP (astrocytic marker; green). As compared to statically cultured cells that predominantly differentiated to neurons (**A-C**), confocal 3D reconstruction of hydro-acoustically actuated cell/scaffold constructs (mechano-electrical stimulation) (**D-F**) showed a multi-phenotypic differentiation behavior, resulting in the formation of a multilayered cellular structure. (**G-L**) Single oblique sections (indicated in **A-F**) from each 3D confocal image of (**G-I**) static and (**J-L**) actuated conditions showing the formation of multi-phenotypic cellular interfaces under the mechano-electrical stimulation (scale bar=100 μm). (**M, N**) Quantitative analysis of confocal images showing the depth-dependent distributions of neuronal and glial cells (**M**) without or (**N**) with the mechano-electrical stimulation. Each graph used three confocal Z-stack images from independent samples. For the mechano-electrical stimulation condition, human neural stem cells (hNSCs) were pre-cultured on the piezoelectric scaffolds for 2 days prior to being subjected to hydro-acoustic actuation (2 hrs/day) for a subsequent 19 days. Cells cultured on the piezoelectric scaffolds without being subjected to hydro-acoustic actuation served as static controls.

To determine the effects of the mechano-electrical stimulation on the cellular interactions between neuronal and glial cells, which will likely lead to the functional

enhancement of the engineered nerve construct, hNSCs that were differentiated by either traditional biochemical factors (biochemically mediated) or mechano-electrical stimulation via the hydro-acoustic actuation of the piezoelectric scaffolds for 3 weeks, were closely examined by confocal microscopy for β3-tubulin, an axonal marker, and GALC, a myelin-associated marker. As expected, the cells differentiated toward both neurons and oligodendrocytes under the biochemically mediated condition, evident from the presence of axonal elongations and a few GALC-positive cell bodies (**Figure 7A-F**, (**Video S3A, B**)). However, no obvious cell-cell interaction between neurons and oligodendrocytes was observed. In contrast, two distinct cellular interactions between neurons and oligodendrocytes were observed under the mechano-electrical stimulation condition. In densely populated regions, β3-tubulin and GALC-positive cells formed a cell colony, where axons were extended throughout the structure (**Figure 7G, H**, (**Video S3C**)). Clearly, the mechano-electrical stimulation induced a cell population in which a greater number of cells differentiated towards oligodendrocytes as compared to that of the biochemically mediated condition. More interestingly, in sparsely populated regions near the vicinity of these dense colonies, a node structure in which GALC-positive extensions wrap around elongated axons, was observed (**Figure 7I, J**, (**Video S3D**)). Closer examination revealed that an oligodendrocytic cell body wraps around an axon and develops a sheath following the axonal extension (**Figure 7K, L**, (**Video S3E**)). As shown in Figures 5 and 6, the static condition, where the cells were statically cultured on the piezoelectric scaffold, did not induce glial differentiation. The results demonstrate that the mechano-electrical stimulation not only promotes multi-phenotypic differentiation of NSCs simultaneously towards neurons and glial cells without biochemical differentiation factors but also induces greater cellular interactions between the different phenotypes for functional maturation.

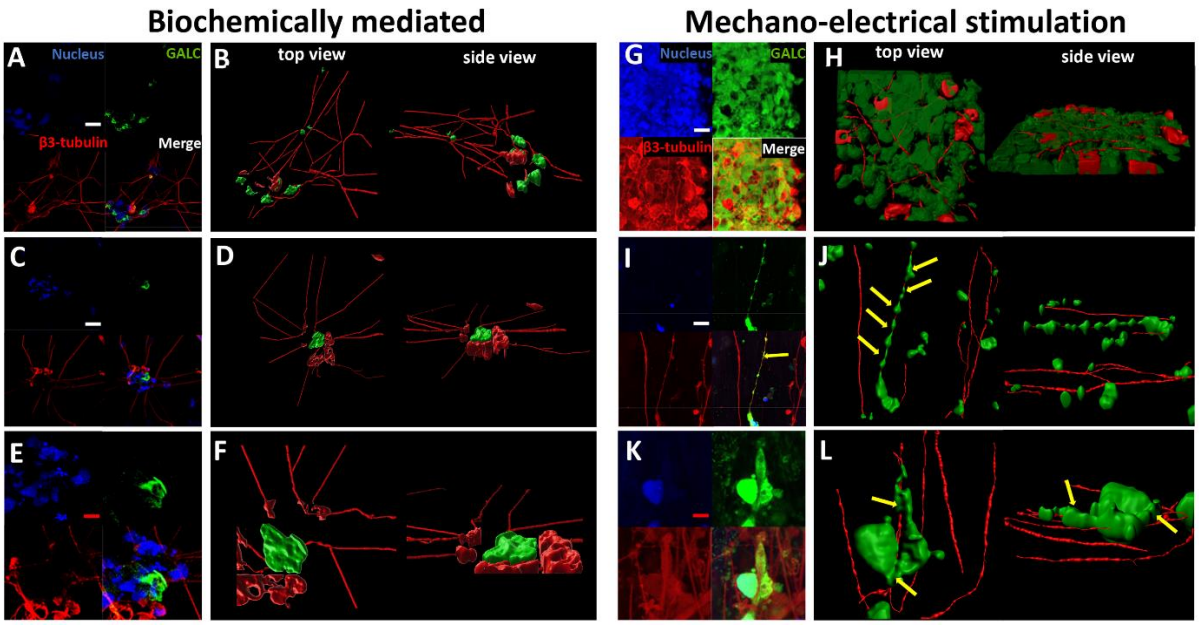


**Figure 7. Cell-cell interactions in the neuron-glial interface derived from a single neural stem cell source *in situ* by piezoelectric P(VDF-TrFE) scaffold-mediated mechano-electrical stimulation.** Confocal images of human neural stem cells (hNSCs) cultured on either (**A-F**) traditional cell culture plate with neural differentiation media (biochemically mediated) or (**G-L**) cultured on electrospun aligned P(VDF-TrFE) scaffolds with neural maintenance media and subjected to the mechano-electrical stimulation for 3 weeks, double-stained with anti-GALC (myelin marker; green) and anti-β3-tubulin (axonal marker; red). Z-stack confocal images (**A, C, E, G, I, K**) were 3D reconstructed by Bitplane Imaris (**B, D, F, H, J, L**) to show interactions between neurons and oligodendrocytes as indicated by yellow arrows (white scale bar=50 μm, red scale bar=5 μm).

Multielectrode array (MEA) measurement was utilized to test whether this morphologically observed, close neuron-glial cell interaction, derived from the application of mechano-electrical stimulation, affects the functionality of the engineered nerve construct. The measurements were conducted on either the cells directly cultured on the cell culture chamber of MEA array with biochemical factors (biochemically mediated) or the cell/piezoelectric scaffold constructs placed on top of MEA with cells facing the array after being statically cultured (static) or hydro-acoustically actuated (mechano-electrical stimulation) (**Figure 8**). Eleven randomly selected electrodes were individually stimulated and action potential induction was monitored in the responding electrodes. Greater connectivity of extracellular neuronal activities was observed in the mechano-electrically stimulated cell/scaffold construct

as compared to those in the biochemically mediated condition or statically scaffold-cultured condition (**Figure 8A-C**). In fact, no electric response was observed in the biochemically mediated condition. When MEA with 10 µm spacing was used instead of that with 200 µm spacing, however, neuronal activities were observed from the biochemically mediated condition, indicating that axonal elongation derived from hNSCs under biochemical mediation is not long enough to bridge across electrodes with a larger gap of 200 µm spacing (**Figure S8A**). Furthermore, the observed neuronal activities of both static and actuated conditions in MEA with 200 µm spacing demonstrate that longer functional neurite outgrowth when hNSCs were cultured on electrospun aligned P(VDF-TrFE) scaffolds with or without the mechano-electrical stimulation as compared to the biochemically mediated condition (**Figure 8B, C**). Significantly higher magnitudes of action potential induction and longer durations of hyperpolarization in the mechano-electrical stimulation condition may indicate a greater number of functional neurons (**Figure 8D, E, S8B**). Moreover, the enhanced interaction between neurons and glial cells under the mechano-electrical stimulation likely led to the enhanced response velocity of the engineered nerve construct (**Figure 8F**). Overall, these results demonstrate that the combination of mechanical and electrical stimulations, derived from the hydro-acoustic activation of the piezoelectric scaffold, synergistically induces the differentiation and maturation of NSCs simultaneously towards all three neural cell types. More importantly, the mechano-electrical stimulation promotes the generation of mature, elongated neurons in the presence of myelinating oligodendrocytes, leading to the formation of functionally competent engineered nerve tissues.

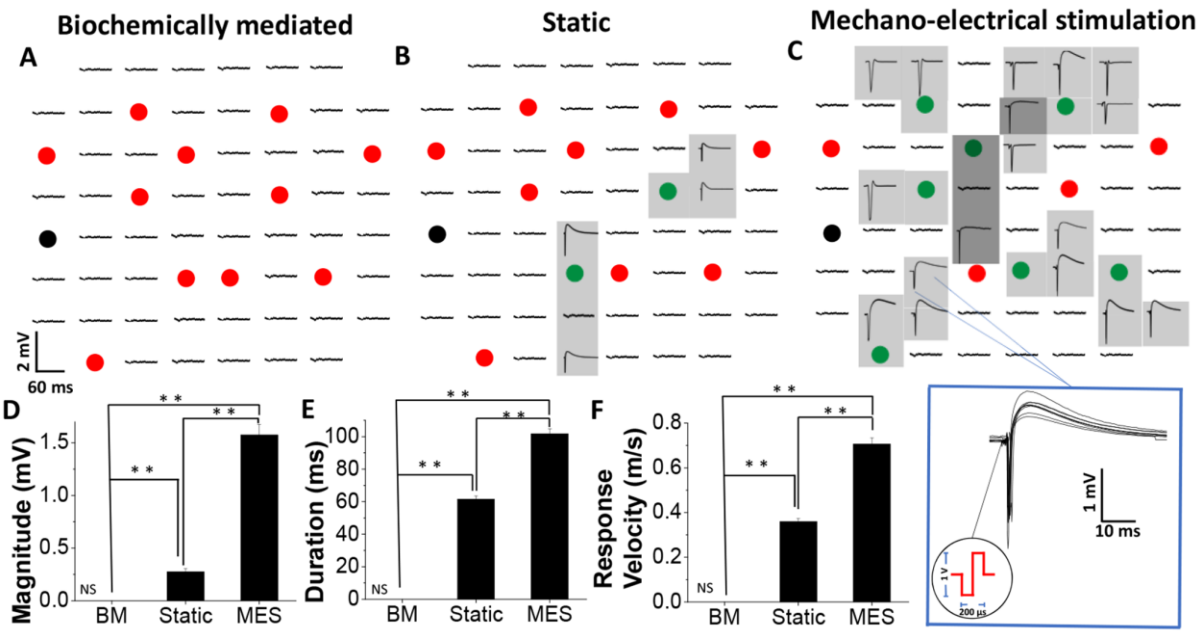


**Figure 8. Functional assessment of engineered neural networks by a multi-electrode array.** Representative connectivity maps of extracellular neuronal activities in the samples where (**A**) hNSCs were cultured directly on a multi-electrode array (MEA) chamber with neural differentiation media (biochemically mediated), or (**B**, **C**) cells were inoculated on electrospun aligned P(VDF-TrFE) scaffolds, and either statically cultured (**B**; static) or hydro-acoustically actuated (**C**; mechano-electrical stimulation), determined by an MEA (60 electrodes with 200 μm spacing). Eleven electrodes (marked by circles in the figure), randomly selected from a total of 60 electrodes, were utilized to stimulate each sample with a biphasic pulse of –500 mV immediately followed by +500 mV for a duration of 200 μs for a total of 10 repetitions (1 stimulation sequence for every two seconds). Green circles indicate the electrodes that elicited cellular responses from nearby electrodes while red circles indicate electrodes without any responses. A black circle indicates an electrode used as ground. Inset (bottom right) shows an example of extracellular neuronal responses from 10 repetitive stimulations with the applied stimulation regimen. Average (**D**) depolarization magnitude, (**E**) response duration, and (**F**) response velocity of biochemically mediated, statically cultured, or mechano-electrically stimulated conditions from the MEA analysis (BM: biochemically mediated, MES: mechano-electrical stimulation, NS: no signal) (n varies with the number of electrodes responded to stimuli; ** denotes the statistical significance of $p < 0.01$; error bars indicate the standard error of the mean).

## 3. Discussion

There are more than 600 neurological diseases caused by genetic disorders, injuries/infections, and aging-related degeneration.[17] These diseases uniquely challenge the quality of life as they typically impair cognitive, sensory, and motor functions. Although there is an exponential increase in the prevalence of such diseases partly due to our aging population, effective treatments are scarcely available. Advances in computational biology and high throughput

technologies have enabled the development of new therapeutics at a fast rate, but these often fail in the late stages of clinical trials. This high attrition rate is largely due to the inefficiency of translating/validating animal-based results to humans.

Due to limitations of human studies, including restricted access to human tissues and unmodifiable experimental conditions for mechanistic studies, various animal models have been developed to gain a better understanding of fundamental pathogenesis and to develop effective treatments of neurological diseases.[18] However, animal models cannot accurately depict all aspects of pathological and clinical features of human diseases due to dissimilarities in genetics and metabolism.[1] Alternatively, researchers have established *in vitro models* to study the underlying molecular mechanisms of neurologic diseases and/or to discover potential pharmacological targets by overcoming the limitations of *in vivo* and *ex vivo* animal models.[2] Despite their simplicity, *in vitro* models enable studying the role of isolated cells of one particular type in a controlled environment that simulates the disease. The use of patient-derived cells in *in vitro* nerve models further demonstrates the significant utility in studying neurological diseases as recent studies discovered a strong relationship between genetics and numerous neurological diseases that were traditionally classified as non-genetic diseases like multiple sclerosis.[19] Many of these *in vitro* models, however, are limited in a single cell type, failing to accurately account for cell-cell interactions among different cell types in the tissue, for example, myelination of neurons by glial cells, which are crucial for nerve physiology. Although several *in vitro* models utilized the co-culture of different cell phenotypes to investigate cell-cell interactions,[20] the cellular structure was limited to two-dimension, failing to resemble the sophisticated 3D structures of the native tissues.

In this regard, this study aimed to develop a piezoelectric material-based strategy to physically stimulate a single source of neural stem cells for the formation of neural tissues, composed of multiple phenotypic cells that are functionally interacting with each other.

Piezoelectric materials have been previously used to enhance neural cell behaviors.[12a] However, those studies were likely unable to utilize the full functionality of piezoelectricity as it requires a dynamic strain to generate physiologically relevant magnitudes of electric potentials necessary to elicit favorable cellular responses. The modified cellular behaviors were attributed to the piezoelectric responses of the PVDF scaffold by cells' contractile forces. Considering minute straining possible from the cell contraction on this relatively stiff material,[15] however, the favorable cellular responses were likely because of intrinsic surface net charges of the material rather than piezoelectric responses. A recent study utilized ultrasound as a mechanical cue to induce the piezoelectric effects from a PVDF membrane and showed anabolic responses from PC12 neuronal cells,[21] The high frequency of mechanical perturbation from ultrasound used in the study, however, does not expect to generate meaningful magnitudes of electrical potentials to affect cellular behaviors. In comparison to these studies, we demonstrated that cells exposed to dynamic mechano-electrical stimulation, mediated by the hydro-acoustic actuation of piezoelectric scaffolds, exhibited significantly enhanced multi-phenotypic differentiation of NSCs, as compared to statically cultured cells on the piezoelectric scaffolds, where the activities of statically cultured cells would be equivalent to those from the aforementioned studies. This was possible by our systematic approach to optimize the piezoelectric and morphological properties of P(VDF-TrFE) nanofibers with thorough material characterization, in order to generate the appropriate electric potential to stimulate neural cells by non-contact mechanical perturbation.

By utilizing these optimized piezoelectric scaffolds, we showed that the mechano-electrical stimulation induces the formation of neural tissue, derived from a single cell source of neural stem cells and composed of all three major neural cell phenotypes including neurons, oligodendrocytes, and astrocytes. Interestingly, the engineered nerve construct formed a 3D organized structure, where a mixed cell layer of oligodendrocytes and astrocytes forms in

immediate proximity to the scaffold surface while a layer of neuronal cells localizes over the glial cells. This phenotypic localization may be due to the differentiation sequence of neural stem cells during embryonic development, where neurons develop first which, in turn, triggers the signaling pathways for the induction of glial cells, including oligodendrocytes and astrocytes.[22] Our data showed that a layer of neurons initially forms on the surface of scaffolds in an early culture period, followed by the formation of the glial cell layer in between the scaffold surface and the neuronal cell layer. Depth-wise confocal imaging did show that there is a population of the cells expressing both neuronal and glial cell markers at the interface of the distinct cell populations, suggesting that the newly proliferating cells at the top surface of the cellular structure would become neurons while the pre-existing cells near the bottom further differentiate towards either type of glial cells under the mechano-electrical stimulation. In contrast, NSCs cultured statically on the piezoelectric scaffolds rarely expressed astrocyte and oligodendrocyte markers, further demonstrating that the mechano-electrical stimulation significantly promotes the oligodendrocytic and astrocytic differentiation of NSCs to form a neural tissue composed of multi-phenotypic cells. Therefore, our technology may overcome the limitations of current *in vitro* models that are restricted to either the single-cell levels or simple co-culture systems of neurons and glial cells without structural elements (as shown in our biochemically mediated condition), failing to accurately account for tissue-level complexity.[23] With interacting cell populations of multiple phenotypes, which are derived from a single stem cell source by the mechano-electrical stimulation, the engineered nerve construct exhibited superior functionalities in neural network connectivity, action potential induction, and response velocity. Overall, these results imply the potential of the platform to create more realistic patient-specific *in vitro* models using patient-derived stem cells for addressing current limitations in the understanding of the pathologies of genetic-associated neurological diseases.

## 4. Conclusion

In summary, a mechano-electrical stimulation strategy built upon a biocompatible piezoelectric scaffold of electrospun aligned P(VDF-TrFE) nanofibers was developed and utilized to enhance the functional development of NSCs. Specifically, a significant enhancement in the multi-phenotypic differentiation of NSCs towards neuron, oligodendrocyte, and astrocyte cell phenotypes was achieved by the synergistic effects of mechanical and electrical stimulations utilizing the piezoelectric material-based technology. The cellular interactions among the different cell populations result in superior neural functionality with an organized 3D structure. These results demonstrate the potential of the piezoelectric material-based technology for patient stem cell-derived nerve tissue formation composed of multiple cell phenotypes with competent tissue functionalities.

## 5. Experimental

*Synthesis and morphological characterization of P(VDF-TrFE) scaffolds*

Various concentrations of P(VDF-TrFE) (70:30 mol%, Solvay Group, France) dissolved in different solvent systems were prepared to produce electrospun nanofibers with a range of fiber diameters, similar to our previous report.[13] 16 wt.% P(VDF-TrFE), dissolved in a solvent system containing a 60/40 volume ratio of N,N-dimethylformamide (DMF) (Sigma Aldrich, St. Louis, MO) to methyl ethyl ketone (MEK) (Sigma Aldrich), was electrospun to produce a fiber diameter of 802 ± 16 nm. 5 wt.% or 7 wt.% P(VDF-TrFE) in DMF: acetone (60: 40 by volume) with the addition of 1 wt.% pyridinium formate (PF) buffer (Sigma Aldrich) prepared for electrospun fiber diameters of 205 ± 28 nm and 498 ± 57 nm, respectively. As the basis for a piezoelectric inactivated control, a solution of 13.5 wt.% of PVDF (Sigma Aldrich) dissolved in the same DMF/acetone/PF solvent system was used. Each solution, magnetically stirred at

1200 rpm for 3 hrs at room temperature until the solution turned clear, was electrospun under optimized conditions of electrospinning distance (10 cm), applied voltage (approximately -15 to -20 kV), and solution feed rate (6 ml $hr^{-1}$), at 23 °C and absolute humidity of approximately 7.6 g $m^{-3}$. Electrospun fibers were collected onto a rotating, grounded wheel rotating at an angular velocity of 47.9 m $s^{-1}$ for various durations to yield scaffolds of aligned fibers having various thicknesses of up to approximately 200 µm. The P(VDF-TrFE) fiber deposits were subsequently annealed at 90 °C for 24 hrs, which was determined from a phase transition analysis described below, to enhance the piezoelectric properties. For piezoelectric inactivation, the PVDF fiber deposits were thermally treated for 1 hr in a rapid thermal annealing oven (Allwin21 Corp, Morgan Hill, CA) at 157 °C, to induce the electroactive- to α-phase transition without causing melting of the fibrous structure, followed immediately by quenching in cold ethanol to preserve the non-piezoelectric α-phase. The morphology of these electrospun scaffolds was characterized using a VEGA3 scanning electron microscope (SEM) (Tescan Brno, Czech Republic).

*Temperature-dependent phase transition analysis of electrospun PVDF nanofibers*

The phase transition temperatures of electrospun P(VDF-TrFE) and PVDF nanofibers were determined using a differential scanning calorimeter (NETZSCH DSC 214 Polyma, Wittelsbacherstraße 42, Germany). DSC curves were acquired by heating a sample (6.9 mg of P(VDF-TrFE) or 5.9 mg of PVDF) from 25 °C to 230 °C at a heating rate of 2.5 °C $min^{-1}$ in air.

*Piezoelectric characterization of electrospun nanofibers*

An MFP-3D Atomic Force Microscopy (AFM) (Asylum Research, Santa Barbara, CA) was used to measure the piezoelectric coefficient of electrospun nanofibers. Briefly, nanofibers of

P(VDF-TrFE) and PVDF were sparsely collected on a gold-coated, thermal-oxide silicon substrate and subjected to single-point piezoresponse force microscopy on individual fibers. AFM imaging mode was first used to identify the location of an individual nanofiber. Five different points were selected on each scanned fiber and the AFM imaging mode was switched to PFM mode where single point voltage-amplitude measurements were conducted. Step voltages from -3 to +3 V were applied across the fiber via the AFM probe (AC240TM, Olympus) to the grounded substrate. The value of $d_{33}$ was calculated by,

$$d_{33} = \frac{A}{VQ} f \ ,$$

where $A$ is the amplitude of the nanofiber in response to the applied voltage ($V$), $Q$ is the quality factor of the AFM probe, and $f$ is the correctional factor derived from a standard periodically poled lithium niobate (PPLN).

For the macroscale electrical output measurement of piezoelectric scaffolds, a cell culture system, based on 3D printed acrylonitrile butadiene styrene (ABS) chambers (**Figure S1A**), was engineered to contain and apply a non-contact hydro-acoustic actuation to induce the piezoelectric effect of the nanofibrous P(VDF-TrFE) scaffold by a subwoofer, used as the vertically translating stage. Each chamber was designed to fit into a well of a standard 6-well tissue culture plate. The subcomponents of the chamber consist of a top and a bottom casing each with silicone o-rings serving to create both fixed points for the scaffold and a mechanical seal when the top and bottom casings are mated with stainless steel screws. The hollow cylindrical nature of the chambers allows the suspension of the scaffold thus promoting an unrestricted region for the scaffold to deflect in response to the indirect mechanical actuation in an aqueous solution (hydro-acoustic waves).

To quantify the voltage generated across the electrospun aligned P(VDF-TrFE) scaffolds or the absence of voltage generated across the thermally inactivated electrospun

aligned PVDF scaffolds, acoustic stimulation was applied onto acellular scaffolds, having a dimension of 45 x 5 $mm^2$, inside the cell culture system. Both sides of the scaffolds were gold-sputtered for electrodes (**Figure S1B**). A hydrophobic poly(styrene-block-isobutylene-block-styrene) (SIBS, Sibstar, Kaneka, Pasadena, TX) coating was applied, via brushing with a 30 wt.% SIBS in toluene (Fisher Scientific, Pittsburgh, PA) solution, on top of the gold-sputtered electrodes to avoid an electrical short circuit. The scaffold, prepared for the electrical output measurement, was assembled into the cell culture chamber, which was placed on the vertical translating platform, and 2 mL of water was added into the center hollow region of the chamber submerging the scaffold. Different magnitudes of strains were applied indirectly to the scaffold by driving various amplitudes of a 3 Hz pulse signal via a function generator that was connected to the subwoofer by an amplifier. The generated voltage across the scaffold was simultaneously measured by an oscilloscope (Pico Technologies, UK). The corresponding strain change was determined by our previously designed cantilever system.[15]

*Cell culture of mouse and human neural stem cells*

C17.2 mouse neural stem cells (mNSCs), derived from the cerebellum of a neonatal mouse,[24] were cultured in high glucose DMEM, supplemented with 10% FBS (VWR, Radnor, PA), 5% horse serum (Gibco, Gaithersburg, MD), 1% sodium pyruvate (Gibco), and 1% penicillin/streptomycin (Mediatech, Manassas, VA).

All experiments involving human stem cells were approved by UC Riverside Institutional Review Board (IRB; HS11-124) and Stem Cell Research Oversight (SCRO; SC20210002) Committee. Human neural stem cells (hNSCs) were derived from well-characterized human induced pluripotent stem cells (hiPSC) using a neural induction medium (Life Technologies, Carlsbad, CA) according to the protocol with modifications.[25] Briefly, hiPSCs cultured in mTeSR1 media (STEMCELL Technology, Canada) were split as cell

clumps onto Geltrex (Fisher Scientific)-coated six-well plates at a density of 2 x $10^4$ cells $cm^{-2}$. After cells reached approximately 25% confluency, the culture medium was switched to the neural induction medium containing Neurobasal medium (Fisher Scientific) and PSC neural induction supplement (Gibco). On Day 7 of neural induction, primitive hNSCs were dissociated with Accutase (Life Technologies) and plated on Geltrex-coated dishes at a density of 3 x $10^4$ cells $cm^{-2}$ in an NSC expansion medium containing 50% Neurobasal medium, 50% Advanced DMEM/F12 (Gibco), and Neural induction supplement. 5 μM ROCK inhibitor (Y27632, R&D Systems, Minneapolis, MN) was used for the first 24 hrs when the hNSCs were split. Cells at passage 4 were used for all experiments.

*Cellular alignment on P(VDF-TrFE) scaffolds with different fiber diameters*

A cell seeding density of 2500 mouse NSCs per $cm^2$ were seeded onto sterile P(VDF-TrFE) scaffolds having average fiber diameters of 200, 500, or 800 nm. The cells were fixed with 4% paraformaldehyde (PFA) after 96 hrs of culture, followed by phalloidin (Alexa Fluor-594, Invitrogen, Carlsbad, CA) staining to visualize their cellular alignment relative to the aligned fiber orientation using an epi-fluorescence microscope (Eclipse Ti, Nikon, Melville, NY). ImageJ software was used to quantify cell alignment, where a line segment was manually drawn on the longest end-to-end of each cell, and its angle of deviation from the average direction of the aligned P(VDF-TrFE) fibers was measured. The quantification involved using 150 cells in 15 different areas from 3 independent samples for each condition.

*The effects of electrical stimulation on cellular behaviors*

A cell culture device was designed to apply direct electrical stimulation to mouse neural stem cells (mNSCs) cultured on the thermally inactivated electrospun aligned PVDF scaffolds. Briefly, gold-sputter coated polystyrene films (15 mm x 5 mm), having a layer of the scaffold

with the same dimensions, were glued to a tissue culture plate with a medical adhesive (Factor II, Inc). A hole was drilled through each well of the tissue culture plate to connect the gold-coated polystyrene film to a function generator. A grounded gold-coated glass coverslip (Thermo Fisher, Waltham, MA) was placed 5 mm above the gold-coated polystyrene film. Different magnitudes of electrical impulses (100, 200, and 300 $mV_{p-p}$), which have similar signal patterns to potential peaks produced from piezoelectrically actuated electrospun aligned P(VDF-TrFE) scaffolds, were applied to cell/scaffold constructs via the function generator. The cell culture system for direct electrical stimulation was sterilized by 70% ethanol and UV light exposure for 30 min and 1 hr, respectively. A cell seeding density of 2500 cells $cm^{-2}$ was used and the cells were pre-cultured for 48 hrs before being subjected to various magnitudes of direct electric fields (2 hrs/day) for the subsequent 3 days. Cells were then fixed in 4% PFA, followed by immunofluorescence staining of neuronal marker (anti-β3-tubulin, Fisher) and counter-staining with phalloidin for actin and DAPI (Sigma) for nucleus. Fluorescence images were taken by the Nikon microscope as described above. The number of total cells and neurons were quantified by counting the DAPI-stained cells (blue) and β3-tubulin-positive cells (green), respectively, using imageJ software.

*Application of electrical, mechanical, or mechano-electrical stimulation on neural stem cells*

Strips of thermally treated P(VDF-TrFE) and PVDF scaffolds (40 x 5 $mm^2$) were prepared, and a layer of hydrophobic SIBS coating was applied to the periphery of the scaffolds to create a 7 mm x 5 mm cell culture area (**Figure S1C**). The scaffolds were assembled within the culture chambers as previously described, followed by 10 kGy X-ray irradiation for sterilization.[26] After sterilization, the cell culture area of each scaffold was pre-wetted with 70% ethanol, washed several times with PBS, and coated overnight with 20% FBS in DMEM. mNSCs were seeded onto each scaffold at a density of 2500 cells $cm^{-2}$. The cell/scaffold constructs were pre-

cultured for 2 days in the growth media as described earlier before being subjected to 1) direct electrical stimulation with peak-to-peak electrical impulses of 200 $mV_{p-p}$ on the cells cultured on thermally treated, thus piezo-inactivated electrospun aligned PVDF scaffolds for 5 days (2 hrs/day) as described in the previous section (pure electrical stimulation (ES) group), 2) hydro-acoustic actuation on the cells cultured on thermally inactivated electrospun aligned PVDF scaffolds for 5 days (2 hrs/day) (pure mechanical stimulation (MS) group), or 3) hydro-acoustic actuation where cells were cultured on piezoelectric electrospun aligned P(VDF-TrFE) for 5 days (2 hrs/day) (mechano-electrical stimulation (MES) group). For the MS and MES groups, the actuation chambers loaded with cell/scaffold constructs were placed in a 6-well plate and subjected to actuation by the vertical translational stage to apply a surface strain of approximately 0.03%. The actuation regimen was experimentally determined to generate 200 $mV_{p-p}$ for an approximately 200 μm thick P(VDF-TrFE) scaffold when actuated at 3 Hz. The cell/scaffold constructs were actuated daily for 2 hrs. Alternatively, the cell/scaffold constructs in the MES group were actuated for 19 days to examine the effects of long-term mechano-electrical stimulation on neural stem cell behaviors. As controls, cells were cultured either in the cell culture system statically or on tissue culture plates for the same duration. After 2 hrs from the last mechanical actuation regimen on the $7^{th}$ or $21^{st}$-day post-cell seeding, cells were subjected to either 4% PFA fixation for immunofluorescence imaging or lysed for gene expression analysis.

Alternatively, hNSCs were also subjected to the mechano-electrical stimulation on the piezoelectric P(VDF-TrFE) scaffolds. Briefly, after sterilizing the cell culture system, the cell culture area of each scaffold was coated with poly-L-ornithine (Sigma Aldrich) for 1 hr, followed by laminin (Thermo Fisher, Waltham, MA) for 2 hrs. Human NSCs were seeded onto each scaffold at a density of 45000 cells $cm^{-2}$. Similar to the mNSC samples, the cell/scaffold constructs were actuated daily for 2 hrs for 19 days after the initial 2 days of the preculture

period. Throughout the pre-culture and actuation duration, the growth media was used. After 2 hrs from the last actuation regimen on the 21st-day post-cell seeding, the samples were subjected to 4% PFA fixation for immunofluorescence imaging. The hNSC/scaffold constructs, cultured in the cell culture system without hydro-acoustic actuation, were used as static controls. Additionally, hNSCs were cultured on poly-L-ornithine and laminin-coated glass slides in the growth media for 48 hrs post-seeding and then in neural stem cell multi-phenotypic differentiation media (neurobasal media with N2 supplement (Gibco), B27 (Gibco), and 1% FBS) for subsequent 19 days. These cells were used as controls for the traditional biochemically mediated neural stem cell differentiation.[27]

*Gene expression analysis*

The effects of electrical, mechanical, or mechano-electrical stimulation on mNSCs after a total culture duration of 7 days were determined at the gene level by quantitative polymerase chain reaction (qPCR). RNA was extracted using an RNeasy Micro Kit (Qiagen, Valencia, CA) followed by cDNA synthesis using an iScript cDNA Synthesis Kit (Bio-Rad, Hercules, CA). Real time-qPCR was performed to determine the gene expression of phenotypic markers (**Table S1**). Raw data were analyzed by the comparative threshold cycle ($C_T$) method using the expression of *Gapdh* as an endogenous control.

*Immunofluorescence imaging*

To characterize the phenotype-specific protein expression of mNSCs towards neuronal or glial cells, mNSCs cultured under the ES, MS, or MES condition for 1 week were subjected to immunostaining with primary antibody markers specific for neurons (β3-tubulin), oligodendrocytes (MBP, Santa Cruz Biotechnology), or astrocytes (EAAT2, Santa Cruz Biotechnology) with an appropriate secondary antibody (m-IgGκ BP-CFL 488, Santa Cruz

Biotechnology). The samples were counterstained with DAPI and phalloidin (Alexa Fluor-594). Alternatively, both mNSCs and hNSCs cultured for 3 weeks with or without the hydro-acoustic actuation were subjected to double-staining with neuronal marker NeuN (Abcam, Cambridge, MA) and astrocytic marker ALDH1L1 (Santa Cruz Biotechnology), NeuN, and oligodendrocytic marker $O_4$ (Sigma Aldrich), or astrocyte marker GFAP (Cell Signaling, Danvers, MA) and $O_4$ to visualize different phenotypic populations of the cells, using a confocal microscope (Zeiss 880 Upright, Zeiss, White Plains, NY). The population and distribution of different phenotypes with respect to the thickness of the cell/scaffold constructs were determined using the ImageJ software. Briefly, 14 z-sectional images from each confocal imaging volume were exported and split into 3 color channels (red, green, and blue). Red or green-positive cells, associated with the protein of interest, were quantified as a percentage of the total cell number (determined by blue-DAPI staining). Three different confocal z-sectional images from 3 independent samples were utilized for each condition.

Furthermore, to examine the cell-cell interaction between oligodendrocytes and neurons, hNSCs either biochemically mediated, or hydro-acoustically actuated for 3 weeks were subjected to double staining with β3-tubulin and GALC (EMD Millipore, Temecula, CA) antibodies for the visualization of neuronal and mature oligodendrocytic cells, respectively. The stained samples were visualized by confocal microscopy and z-stack images were subjected to 3D reconstruction using Bitplane Imaris software (Oxford Instruments, Concord, MA).

*Functional assessment of NSC-derived, engineered neural tissue by the multielectrode array*

Multielectrode array (MEA, MultiChannel Systems, Germany) was utilized to assess the neuronal activities of the engineered nerve constructs, derived from biochemically mediated, statically cultured, and hydro-acoustically actuated hNSCs for 3 weeks. The MEA array

consists of 60 titanium nitride (TiN) electrodes with 30 μm in diameter and 200 μm spacing. hNSCs were directly cultured in the MEA chamber for the biochemically mediated differentiation condition while statically cultured or mechano-electrically stimulated samples, where cells were cultured on electrospun aligned P(VDF-TrFE) scaffolds, were placed on MEA with the cell-cultured side facing the MEA electrodes. The samples were electrically stimulated by 11 randomly selected electrodes separately. A biphasic electrical stimulation of -500 mV, immediately followed by +500 mV with an overall duration of 200 μs was utilized. Each electrical stimulus was repeated 10 times with a 2 s time gap between stimuli. The system was placed in an incubator at 37 ℃ with 5% $CO_2$ during the measurements.

Electrical signals between 20 ms pre-stimulus and 200 ms post-stimulus were acquired from all electrodes (MC Rack, MultiChannel Systems). In order to remove artifacts from the applied electrical stimulation, an approach similar to a template subtraction method was used,[28] where raw signals from the electrodes away from the stimulation electrode, without any distinct spike, were averaged and this average was subtracted from all channels. At least 3 independent samples for each condition were subjected to MEA analysis.

*Statistical analysis*

Statistical analysis was performed with at least three biologically independent samples and represented as an average ± standard deviation or standard error of the mean. The data were subjected to one-way ANOVA with Tukey's post-hoc test using the SPSS software (IBM) to determine statistical significance ($p < 0.05$).

**Supporting information**

Supplementary Information is available from the online version or from the author.

**Acknowledgments**

YT, GI, and KL equally contributed to this work. The work was supported by the National Science Foundation (CBET-1805975), the Creative Materials Discovery Program through the National Research Foundation of Korea funded by the Ministry of Science and ICT (2018M3D1A1057844), and UC Riverside and Korea Institute of Materials Science (Research Program PNK7280) through UC-KIMS Center for Innovative Materials for Energy and Environment.

**Data Availability**

The raw/processed data required to reproduce these findings cannot be shared at this time as the data also forms part of an ongoing study.

## References


[1] A. Denic, A. J. Johnson, A. J. Bieber, A. E. Warrington, M. Rodriguez, I. Pirko, *Pathophysiology* **2011**, 18, 21.

[2] B. J van der Star, D. Ys Vogel, M. Kipp, F. Puentes, D. Baker, S. Amor, *CNS & Neurological Disorders-Drug Targets (Formerly Current Drug Targets-CNS & Neurological Disorders)* **2012**, 11, 570.

[3] A. W. English, G. Schwartz, W. Meador, M. J. Sabatier, A. Mulligan, *Developmental neurobiology* **2007**, 67, 158.

[4] A. Gärtner, V. Staiger, *Proceedings of the National Academy of Sciences* **2002**, 99, 6386.

[5] J. Huang, Z. Ye, X. Hu, L. Lu, Z. Luo, *Glia* **2010**, 58, 622.

[6] a) C. E. Schmidt, V. R. Shastri, J. P. Vacanti, R. Langer, *Proceedings of the National Academy of Sciences* **1997**, 94, 8948; b) H. Sontheimer, *Glia* **1994**, 11, 156.

[7] S. Y. Park, J. Park, S. H. Sim, M. G. Sung, K. S. Kim, B. H. Hong, S. Hong, *Advanced materials* **2011**, 23.

[8] R. V. Sharma, M. W. Chapleau, G. Hajduczok, R. E. Wachtel, L. J. Waite, R. C. Bhalla, F. M. Abboud, *Neuroscience* **1995**, 66, 433.

[9] a) Y. Shapira, V. Sammons, J. Forden, G. F. Guo, A. Kipp, J. Girgulis, T. Mishra, J. D. de Villers Alant, R. Midha, *Neurosurgery* **2019**, 85, 156; b) W. Jiang, Y. Wang, J. Tang, J. Peng, Y. Wang, Q. Guo, Z. Guo, P. Li, B. Xiao, J. Zhang, *Scientific reports* **2016**, 6, 22773.

[10] a) C. A. Angeli, M. Boakye, R. A. Morton, J. Vogt, K. Benton, Y. Chen, C. K. Ferreira, S. J. Harkema, *N Engl J Med* **2018**, 379, 1244; b) K. Saha, A. J. Keung, E. F. Irwin, Y. Li, L. Little, D. V. Schaffer, K. E. Healy, *Biophysical journal* **2008**, 95, 4426.

[11] a) Y. S. Lee, T. L. Arinzeh, *Tissue Eng Pt A* **2012**, 18, 2063; b) C. Ribeiro, V. Sencadas, D. M. Correia, S. Lanceros-Mendez, *Colloid Surface B* **2015**, 136, 46.

[12] a) P. Aebischer, R. F. Valentini, P. Dario, C. Domenici, P. M. Galletti, *Brain research* **1987**, 436, 165; b) Y. S. Lee, S. L. Wu, T. L. Arinzeh, M. B. Bunge, *Biotechnol Bioeng* **2017**, 114, 444.

[13] G. Ico, A. Showalter, W. Bosze, S. C. Gott, B. S. Kim, M. P. Rao, N. V. Myung, J. Nam, *Journal of Materials Chemistry A* **2016**, 4, 2293.

[14] G. T. Christopherson, H.-Q. Song H Fau - Mao, H. Q. Mao, *Biomaterials* **2009**, 30, 556.

[15] G. Ico, A. Myung, B. S. Kim, N. V. Myung, J. Nam, *Nanoscale* **2018**, 10, 2894.

[16] W. Steinmann, S. Walter, G. Seide, T. Gries, G. Roth, M. Schubnell, *Journal of Applied Polymer Science* **2011**, 120, 21.

[17] M. A. Faghihi, S. Mottagui-Tabar, C. Wahlestedt, *Expert review of molecular diagnostics* **2004**, 4, 317.

[18] M. Bradl, C. Linington, *Brain pathology* **1996**, 6, 303.

[19] P. Khankhanian, T. Matsushita, L. Madireddy, A. Lizée, L. Din, J. M. Moré, P.-A. Gourraud, S. L. Hauser, S. E. Baranzini, J. R. Oksenberg, *BMC medical genetics* **2015**, 16, 55.

[20] a) Y. Pang, B. Zheng, S. L. Kimberly, Z. Cai, P. G. Rhodes, R. C. S. Lin, *Brain and behavior* **2012**, 2, 53; b) E. V. Jones, D. Cook, K. K. Murai, in *Astrocytes*, Springer **2012**, p. 341.

[21] M. Hoop, X. Z. Chen, A. Ferrari, F. Mushtaq, G. Ghazaryan, T. Tervoort, D. Poulikakos, B. Nelson, S. Pane, *Scientific reports* **2017**, 7, 4028.

[22] F. D. Miller, A. S. Gauthier, *Neuron* **2007**, 54, 357.
[23] S. Geuna, S. Raimondo, F. Fregnan, K. Haastert-Talini, C. Grothe, *The European journal of neuroscience* **2016**, 43, 287.
[24] a) M. Li, K. S. Tsang, S. T. Choi, K. Li, P. C. Shaw, K. F. Lau, *Chembiochem* **2011**, 12, 449; b) E. Y. Snyder, D. L. Deitcher, C. Walsh, S. Arnoldaldea, E. A. Hartwieg, C. L. Cepko, *Cell* **1992**, 68, 33.
[25] M. Maldonado, L. Y. Wong, C. Echeverria, G. Ico, K. Low, T. Fujimoto, J. K. Johnson, J. Nam, *Biomaterials* **2015**, 50, 10.
[26] E. Eljarrat‐Binstock, A. Bentolila, N. Kumar, H. Harel, A. J. Domb, *Polymers for advanced technologies* **2007**, 18, 720.
[27] D. Joung, V. Truong, C. C. Neitzke, S. Z. Guo, P. J. Walsh, J. R. Monat, F. Meng, S. H. Park, J. R. Dutton, A. M. Parr, M. C. McAlpine, *Adv Funct Mater* **2018**, 28.
[28] T. Hashimoto, C. M. Elder, J. L. Vitek, *Journal of neuroscience methods* **2002**, 113, 181.

## Table of contents

Youyi Tai[1#], Gerardo Ico[1#], Karen Low[1#], Junze Liu[1], Tanvi Jariwala[1], David Garcia-Viramontes[1], Kyu Hwan Lee[2], Nosang V. Myung[3], B. Hyle Park[1], Jin Nam[1]*

**Formation of 3D self-organized neuron-glial interface derived from neural stem cells via mechano-electrical stimulation**

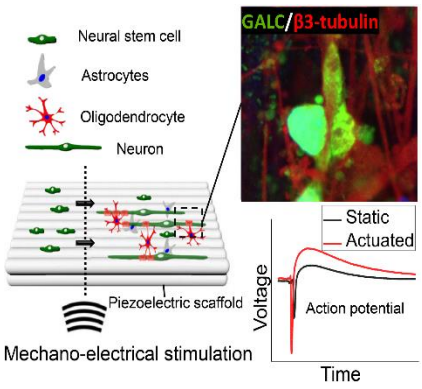


A piezoelectric material is utilized to electrically stimulate neural stem cells under mechanical perturbation. This mechano-electrical stimulation induces multiphenotypic differentiation of neural stem cells simultaneously towards neurons and glial cells, resulting in enhanced neural functionality including the induction of neuronal-glial interaction and enhancement of neural cell functionality.

Click here to access/download
**Supporting Information**
Video_S1.zip

Click here to access/download
**Supporting Information**
Video_S2.zip

Supporting Information Video S3

Click here to access/download
**Supporting Information**
Video_S3.zip

Note to editor